HMGA2 knockdown alleviates the progression of nonalcoholic fatty liver disease (NAFLD) by downregulating SNAI2 expression.

Jing Sun a,* , Xiuli Jin a , Xinhe Zhang a , Birong Zhang b

a Department of Gastroenterology, the First Hospital of China Medical University, Shenyang, Liaoning Province, People's Republic of China

b Systems Immunity Research Institute, Cardiff University School of Medicine, Cardiff University, Cardiff, UK

ABSTRACT

Non-alcoholic fatty liver disease (NAFLD) is a complex disease that is considered as the next major health epidemic with alarmingly increasing global prevalence. To explore the pathogenesis of NAFLD, data from GSE118892 were analyzed. High mobility group AT-hook 2 (HMGA2), a member of the high mobility group family, is declined in liver tissues of NAFLD rats. However, its role in NAFLD remains unknown. This study attempted to identify the multiple roles of HMGA2 in NAFLD process. NAFLD was induced in rats using a high-fat diet (HFD). In vivo, HMGA2 knockdown using adenovirus system attenuated liver injury and liver lipid deposition, accompanied by decreased NAFLD score, increased liver function, and decreased CD36 and FAS, indicating the deceleration of NAFLD progression. Moreover, HMGA2 knockdown restrained liver inflammation by decreasing the expression of related inflammatory factors. Importantly, HMGA2 knockdown attenuated liver fibrosis via downregulating the expression of fibrous proteins, and inhibiting the activation of TGF-β1/SMAD signaling pathway. In vitro, HMGA2 knockdown relieved palmitic acid (PA)-induced hepatocyte injury and attenuated TGF-β1-induced liver fibrosis, consistent with in vivo findings. Strikingly, HMGA2 activated the transcription of SNAI2, which was evidenced by the dual luciferase assays. Moreover, HMGA2 knockdown largely downregulated SNAI2 levels. Indeed, SNAI2 overexpression effectively blocked the inhibitory effect of HMGA2 knockdown on NAFLD. Totally, our findings reveal that HMGA2 knockdown alleviates the progression of NAFLD by directly regulating the transcription of SNAI2. HMGA2 inhibition may emerge as a potential therapeutic target for NAFLD.

1. Introduction

Nonalcoholic fatty liver disease (NAFLD), a hepatic manifestation of metabolic syndrome, is considered to be currently the most common chronic liver disease [1]. As the increased prevalence of obesity, the incidence of NAFLD has been increasing rapidly worldwide [2]. NAFLD can be divided into simple non-alcoholic fatty liver (NAFL) where only hepatic steatosis is observed, and non-alcoholic steatohepatitis (NASH) where intralobular inflammation, hepatocyte ballooning and hepatic steatosis are observed [3]. In particular, NASH is a progressive disease that may contribute to liver cirrhosis and hepatocellular carcinoma [4]. At present, the principal treatments for NAFLD are diet, exercise and pharmacological therapy [5]. The process and pathogenesis of NAFLD are extremely complex and multifactorial [6]. However, there is a lack of consensus on the most useful and appropriate pharmacological therapy for NAFLD. Therefore, it is necessary to elucidate the underlying molecular mechanisms in the progression of NAFLD and develop new therapeutic targets for the early diagnosis and precise intervention of NAFLD.

HMGA2 (High mobility group AT-hook 2), a non-histone small molecule protein belonging to the HMGA family, is regarded as an important regulator of cell growth and differentiation [7]. It has been thought that HMGA2 plays a critical role in adipogenesis and is directly involved in adipose tissue

development and obesity [8]. Moreover, HMGA2, as an oncofetal protein, is associated with the progression of many malignancies including ovarian cancer, colon cancer, hepatocellular carcinoma and other types of cancer [7,9–11]. Accumulating advances have confirmed that HMGA2 drives inflammation pathways by enhancing the levels of pro-inflammatory cytokines, thereby promoting poorly differentiated stem cell phenotypes, tumor progression and refractory diseases [12–14]. Recently, HMGA2 has also been found to participate in advanced disease fibrosis [15]. Besides, HMGA2 is implicated in epithelial-to-mesenchymal transition (EMT) of fibrosis through TGF-β1 signaling pathway [16]. Notably, analysis of the GEO database suggested that HMGA2 expression was significantly down regulated in rats fed a high-fat diet (HFD) relative to normal rats, indicating that HMGA2 may exert a vital role in the development of NAFLD. However, this hypothesis requires further confirmation.

Zinc finger transcription factor SNAI2 (or SLUG) is a member of the SNAIL family and contains an N-terminated snag domain and a C-terminated DNA binding domain [17]. A considerable number of studies have investigated that SNAI2 triggers EMT and orchestrates biological processes that are essential for tissue development and tumorigenesis [18–20]. For instance, SNAI2 promoted liver lipogenesis, fatty liver disease and type 2 diabetes [21]. Recent studies have reported that HMGA2 positively regulates the expression of SNAI2 by directly binding to the region of the SNAI2 promoter [18,22]. Accordingly, whether HMGA2 modulates the transcription of SNAI2 and then affects the process of NAFLD remains to be further analysis.

The present study aims to verify the potential role of HMGA2 in the progression of NAFLD in vivo and in vitro, and further reveal the regulatory mechanism of HMGA2 and SNAI2 in NAFLD.

2. Materials and methods

2.1. Bioinformatics analysis

The gene expression profile (GSE118892) containing control samples and NAFLD samples was selected and downloaded from the GEO database of the NCBI for further analysis. The dataset was normalized and log2 transformed to filter out DEGs of the dataset. The filtering conditions were as follows: |log2-fold change| > 1 and adjusted P-value <0.05. Heat map showed DEGs expression profile. Track showed the expression and chromosomal distribution of DEGs. KEGG pathway and GO enrichment analyses were used to identify the significant pathways. In addition, chordal graph analysis of DEGs on several pathways.

2.2. Construction of adenovirus vector

The shRNA targeting rat HMGA2 sequence (GCAAGAGUCCGCAGAGGAAGA) or its negative control was inserted into pShuttle-CMV vector (Fenghui Biotechnology, Changsha, China), respectively. Adenovirus-carrying shHMGA2 was produced in HEK293T cells.

2.3. Establishment of HFD model in SD rats

All animal experiments were authorized through the Animal Ethics Committee of Shenyang Medical University. After adaptation, rats (8- week-old male) were selected and randomly divided into 4 groups (each group, n = 6). Control group was fed a normal diet for 14 weeks. HFD group was fed a high-fat diet (60 kcal% fat) for 14 weeks. HFD + shRNANC group and HFD + shRNA-HMGA2 group were also fed a high-fat diet for 14 weeks. At the 10th week of HFD feeding, 5 × 109 pfu (50 μl) shRNA-NC adenovirus (HFD + shRNA-NC group) or 5 × 109 pfu (50 μl) shRNA-HMGA2 adenovirus (HFD + shRNA-HMGA2 group) were injected into the tail vein, respectively. Rats was sacrificed after 14 weeks of HFD feeding, liver tissues and blood were collected for further experiments.

2.4. Cell culture and treatment

HepG2 and LX-2 cells were obtained from the Procell (Wuhan, China) and iCell (Shanghai, China), respectively. Cells were seeded on 6- well plates and cultured in MEM (Solarbio, Beijing, China) with 10% fetal bovine serum (Tianhang Biotechnology, Zhejiang, China) at 37 ◦C and 5% CO2.The siRNA targeting human HMGA2 sequence (CCUAAGAGACCCAGGGGAATT) was transfected to cells by using Lipofectamine 3000 (Invitrogen, Carlsbad, CA, USA). Then cells were incubated overnight and transfected with siHMGA2. After 24 h, transfected HepG2 cells were treated with 400 μmol/l PA and LX-2 cells were treated with 10 ng/ml TGF-β1 for subsequent experiments.

2.5. Determination of biochemical parameters

After 10 and 14 weeks of HFD feeding, the body weight and food intake of each rat were determined. Moreover, insulin tolerance test (ITT) and intraperitoneal glucose tolerance test (IGTT) were utilized to measure blood glucose levels. Briefly, in IGTT experiment, rats were fasted for 6 h and injected with glucose (2 g/kg, intraperitoneally). Blood samples were collected from the caudal vein to measure blood glucose concentrations at 0, 30, 60, 90, and 120 min after glucose injection. In ITT experiment, rats were fasted for 12 h and injected intraperitoneally with 0.75 U insulin. Blood samples were collected from the caudal vein and blood glucose levels were measured at 0, 30, 60, 90, and 120 min after insulin injection. Besides, the activities of aspartate transaminase (AST) and alanine transaminase (ALT) in serum were detected by AST and ALT Assay Kits (Jiancheng Bioengineering Institute, Nanjing, China).

2.6. Real-time PCR

RNA was purified and cDNA was synthesized using BeyoRT II M-MLV reverse transcriptase (Beyotime, Shanghai, China). The real-time PCR were performed using a SYBR green qPCR Kit (Solarbio) via ExicyclerTM96 (BIONEER, Korea) real-time system. β-actin was used as the endogenous control. Relative expression was presented using the $2^{-\Delta\Delta Ct}$ method. The primers were listed in Table 1.

2.7. Western blot

Proteins were isolated by a modified RIPA lysis buffer with PMSF (1 mmol/l, Beyotime). Protein concentration was estimated using a BCA protein concentration Assay Kit (Beyotime). Lysates were run on a 10% SDS-PAGE (Solarbio) and transferred to a polyvinylidene difluoride membrane (Millipore, Billerica, MA, USA). After 5% blocking, HMGA2 (1:1000, A2972, Abclonal, Wuhan, China), SNAI2 (1:1000, A5243, Abclonal), FASN (1:1000, A0461, Abclonal), CD36 (1:1000, DF6479, Affinitiy, Changzhou, China), TGF-β1 (1:1000, AF1027, Affinitiy), SMAD2/3 (1:1000, A18674, Abclonal), p-SMAD2/3 (1:1000, AP0548, Abclonal), α-SMA (1:3000, 14,395–1-AP, Proteintech, Wuhan, China), Collagen I (1:500, A5786, Abclonal) primary antibodies were added and incubated overnight at 4 ◦C. Membranes were then incubated with secondary antibodies (goat anti-rabbit IgG-HRP, 1:5000, Beyotime) at 37 ◦C for 45 min. The blot signals on the membrane were visualized with ECL reagents (Beyotime) and data quantification was measured by Gel Pro-Analyzer software.

Table 1 -The information of real-time quantitative PCR primers.

Name	Forward sequence (5′-3′)	Reverse sequence (5′-3′)
Rat HMGA2	CAGCCGTCCACATCAGC	GCCTTTGGGTCTTCCTCT
Rat CD36	CAAAGAATAGCAGCAAGAT	CAGTGAAGGCTCAAAGAT
Rat FASN	CCGCCAGAGCCCTTTGTT	CCACGATGCCACCACGAA
Rat TNF-α	CGGAAAGCATGATCCGAGAT	AGACAGAAGAGCGTGGTGGC
Rat IL-6	CAGCCACTGCCTTCCCTA	TTGCCATTGCACAACTCTTT
Rat IL-1β	TTCAAATCTCACAGCAGCAT	CACGGGCAAGACATAGGTAG
Rat MCP-1	TGTCCCAAAGAAGCTGTA	TCAAAGGTGCTGAAGTCC
Homo HMGA2	ACTTCAGCCCAGGGACA	GTGGCTTCTGCTTTCTTTT
Homo TNF-α	GAGTGACAAGCCTGTAGCC	AAGAGGACCTGGGAGTAGAT
Homo IL-6	GTCCAGTTGCCTTCTCCC	GCCTCTTTGCTGCTTTCA
Homo IL-1β	TATTACAGTGGCAATGAGG	ATGAAGGGAAAGAAGGTG
Homo MCP-1	CTCGCTCAGCCAGATGC	TCGGAGTTTGGGTTTGC

2.8. Hematoxylin and eosin (H&E) staining and NAFLD activity score (NAS)

Rat liver tissues were fixed, embedded in paraffin and sectioned into 5 μm-thick slices. Then sections were dewaxed and rehydrated. Finally, sections were stained with hematoxylin for 5 min and eosin for 3 min. Images were captured by a microscope (Olympus, Japan). The histoogical features including steatosis, lobular inflammation and hepatocellular ballooning were examined. A score system was utilized to evaluate each feature and calculate scores of all the histological features namely NAFLD activity score (NAS) [23]. Besides, liver index (liver index = liver wet weight/body weight×100%) was measured.

2.9. Immunohistochemical staining

Rat liver tissues were fixed and embedded in paraffin. After sections were dewaxed and rehydrated, the endogenous peroxidase activity was blocked with 3% H2O2. Primary antibodies (HMGA2, 1:100, A2972, Abclonal; α-SMA, 1:100, 14,395–1-AP, Proteintech; Collagen I, 1:100, A5786, Abclonal) were incubated at 4 ◦C overnight, followed by secondary goat anti-rabbit IgG-HRP (1:500, ThermoFisher, Pittsburgh, PA, USA) for 1 h at 37 ◦C. The positive staining was visualized using DAB (MXB® Biotechnology, China). Cell nuclei were stained with hematoxylin (Solarbio). Images were

2.10. Oil red O staining

Rat liver tissues or HepG2 cells were fixed in cell ORO fixative for 25 min and washed with PBS. Then sections were stained with Oil Red O solution (Leagene Biotechnology, Beijing, China) for 15 min. The redstained lipid droplets were visualized and photographed under a microscope.

2.11. Lipids detection

According to the manufacturer's protocol, triglycerides (TG) and total cholesterol (TC) levels were determined using Triglyceride Kit (Jiancheng Bioengineering Institute) and Total Cholesterol Kit (Jiancheng Bioengineering Institute), respectively.

2.12. Immunofluorescence staining

Immunofluorescence staining was employed to evaluate expression of CD68 in rat liver tissues and α-SMA in LX-2 cells. Tissues were embedded in paraffin and soaked in PBS. Besides, cells were fixed with 4% paraformaldehyde and permeabilized using 0.1% Triton X-100, then 1% BSA was added and incubated at room temperature for 15 min. Primary antibodies (CD68, 1:300, GB11067, Servicebio, Wuhan, China; α-SMA, 1:100, 14,395–1-AP, Proteintech) were added and incubated overnight at 4 ◦C. Subsequently, secondary antibody goat anti-rabbit IgG-Cy3 (1:200) was added and incubated for 1 h at room temperature. The sections were counterstained with DAPI and images were acquired under a microscope.

2.13. Masson staining and fibrosis grading

*R*at liver tissues were fixed and embedded in paraffin. Then slides were dewaxed in xylene. The nuclei were stained with hematoxylin for 6 min and the cytoplasm was stained with Ponceau acid fuchsin staining buffer for 1 min. Then 1% phosphomolybdate solution was added and treated for 5 min, and re-stained with Aniline blue for 5 min. Finally, the slices were dehydrated again and the staining was obtained by a microscope.

For Fibrosis Grading, 0 = None; 1 = Perisinusoidal or periportal; 2 = Perisinusoidal and portal/periportal; 3 = Bridging fibrosis; 4 = Cirrhosis [23]

2.14. Sirius red staining

Sirius Red staining was also employed to detect fibrosis in the liver. In brief, the embedded tissue was dewaxed in xylene and ethanol. The sections were stained with Sirius Red solution (Solarbio) for 5 min and then the staining was obtained by a microscope.

2.15. Elisa

Samples of tissue or cells were lysed, and protein concentration was estimated using a BCA protein concentration Assay Kit (Beyotime). Then ELISA was performed, according to the instructions of the respective ELISA Kit (MULTI SCIENCE, Hangzhou, China). With the standard concentration as the vertical coordinate and the calibrated OD value as the horizontal coordinate, the corresponding concentration can be calculated according to the standard curve.

2.16. Luciferase reporter gene assays

SNAI2 promoter sequence was cloned into a pGL-3-basic Firefly luciferase reporter vector (Generalbiol, Chuzhou, China), and cotransfected with the HMGA2 overexpression or vector plasmid into HEK293 cells. pRL-TK Renilla served as control plasmid. After transfection for 48 h, cells were collected to detect the luciferase activity. Firefly and Renilla luciferase activities were determined with Synergy H1 (BIOTEK, VT, USA), and the ratio of Firefly and Renilla luciferase was calculated.

2.17. *Statistical analysis*

All statistical analyses were performed using GraphPad Prism 8.0 (GraphPad, Inc., USA). Student's t-test was used to analyze the differences between two groups. Comparison of multi-groups (>2) was performed using a one-way or two-way analysis of variance followed by Bonferroni test. Pathological score was performed using non-parametric test. The data were presented as the mean ± SD. $P < 0.05$ was considered to be statistically significant.

3. Results

3.1. Transcriptomic analysis of DEGs in NAFLD rats in GEO database

Firstly, we downloaded the data from GEO database and analyzed DEGs in NAFLD rats by hierarchical clustering. The heatmap showed the mRNA expression levels in NAFLD rats and the pie chart showed the number of DEGs (Fig. 1A-B). Then we evaluated the expression and chromosomal distribution of DEGs, as reflected in Fig. 1C, HMGA2 was downregulated in NAFLD rats compared to controls. In addition, we performed GO enrichment analysis. As indicated, genes were significantly enriched in glomerular mesangium development in biological process (BP), spanning component of plasma membrane in cellular component (CC), and G protein-coupled neurotransmitter receptor activity in molecular function (MF) (Fig. 1D). KEGG enrichment analysis exhibited that most genes were significantly enriched in Neuroactive ligand-receptor interaction and Human T-cell leukemia virus 1

infection (Fig. 1E). Moreover, we analyzed the enriched DEGs in several pathways during KEGG analysis, as shown in chordal graph (Fig. 1 F). Totally, according to the above analysis of DEGs, HMGA2 was screened out as the target gene in NAFLD rats.

3.2. HMGA2 knockdown improved insulin sensitivity in NAFLD rats

We assessed the changes of liver tissues in HFD-fed rats and normal rats by H&E staining, and the analysis suggested that liver tissues of the HFD rats exhibited significant steatosis, hepatocyte ballooning and lobular inflammation as compared to the controls, implying that HFD fed rats displayed the characteristics of NAFLD (Fig. 2A). Next, an HFD model in rats was induced to explore the function of HMGA2 in the progression of NAFLD. We examined the expression pattern of HMGA2 in rat liver tissues. As indicated by results of real-time PCR and western blot, HMGA2 was at markedly lower levels in the HFD-fed rats (Fig. 2B). Likewise, the above results were further ascertained by immunohistochemical staining (Fig. 2C). Taken together, these observations imply that HMGA2 may participate in the progress of NAFLD and multiple roles of HMGA2 are emphatically identified in subsequent analysis.

Further, an adenoviral vector carrying shRNA targeting HMGA2 in HFD rats was established (Fig. 2D) and HMGA2 knockdown efficiency was detected by real-time PCR and western blot (Fig. 2E). Then the biological characteristics of HMGA2 knockdown-treated rats in the presence of HFD stress were monitored. Our data showed that after 14 weeks of feeding, the HFD group had significantly higher body weight and lower food intake than the rats with normal chow diet, indicating that HFD-fed rats developed obesity. Surprisingly, these changes were reversed in rats injected with shRNA-HMGA2 (Fig. 2F-G). As observed, results of ITT experiment indicated that blood glucose levels decreased rapidly and then slowly. In IGTT experiment, blood glucose levels first increased and then decreased. After 10 weeks of feeding, the area under curve (AUC) of blood glucose in the HFD group, HFD + shRNA-NC group and HFD + shRNA-HMGA2 group was obviously larger than that of the controls, suggesting that these three groups developed distinct insulin resistance (Fig. 2H-I). Dramatically, after 14 weeks of feeding, results of ITT and IGTT experiments confirmed that HMGA2 knockdown notably downregulated blood glucose levels to near-normal levels (Fig. 2J-K), as demonstrated by a reduction in their AUC (Fig. 2H-K), implying that HMGA2 knockdown ameliorated insulin and blood glucose tolerance of NAFLD rats.

Overall, these findings reveal that knocking down HMGA2 suppresses obesity and improves insulin sensitivity in NAFLD rats, indicating that knockdown of HMGA2 may show protective effects in NAFLD process.

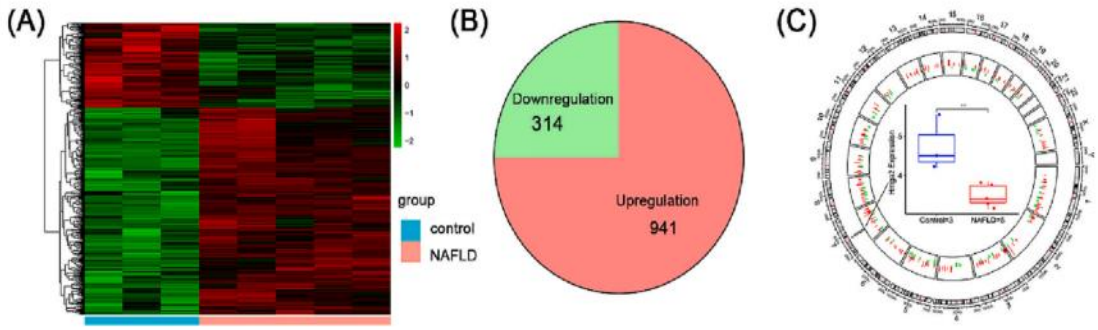

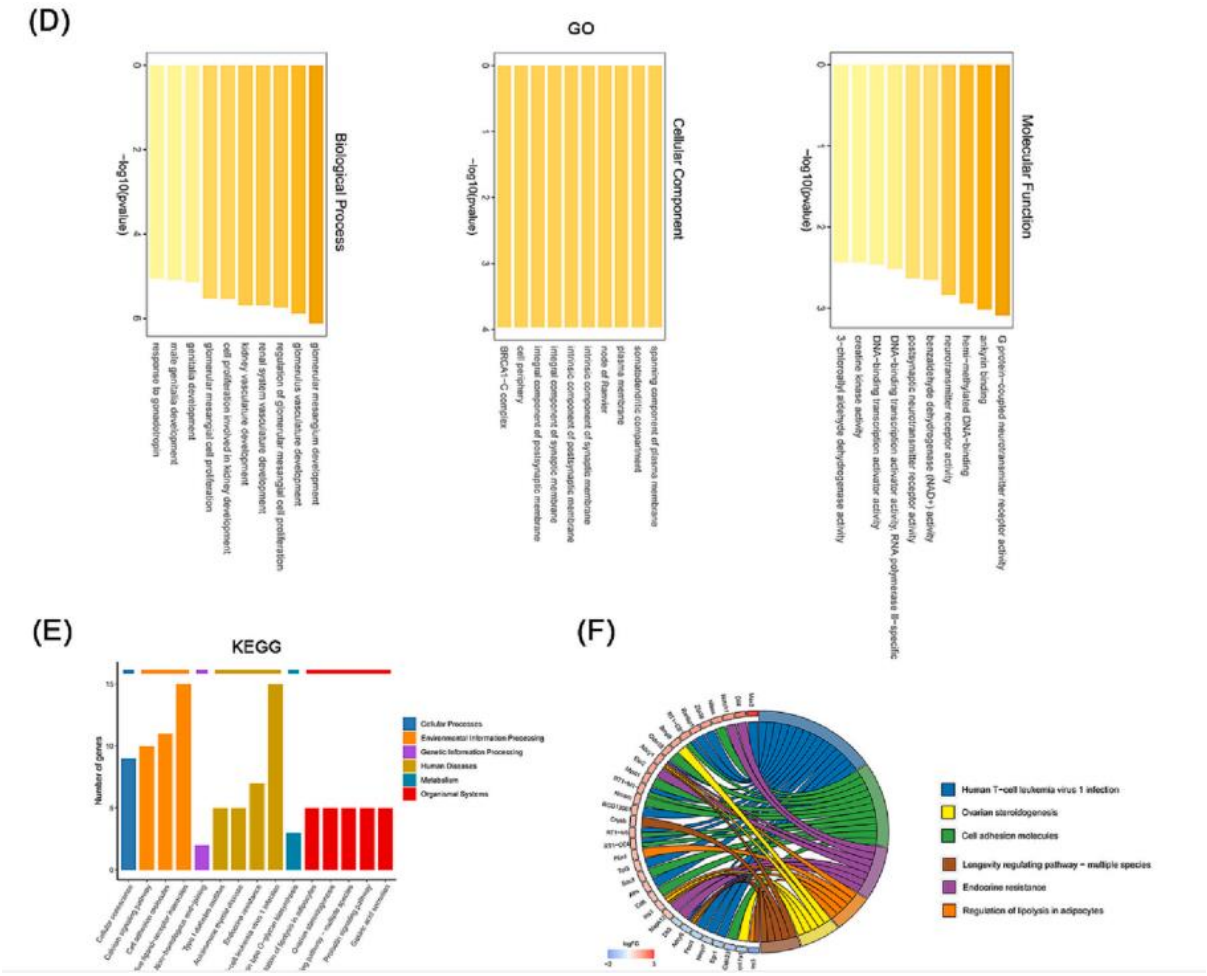

Fig. 1. Transcriptomic analysis of DEGs in NAFLD rats in GEO database. (A) DEGs in NAFLD rats according to GEO database. (B) The pie chart showed the number of DEGs. (C) The expression and chromosomal distribution of DEGs. (D) GO analysis of DEGs. (E) KEGG analysis of DEGs. (F) Chordal graph of DEGs enriched in six kinds of pathways during KEGG analysis.

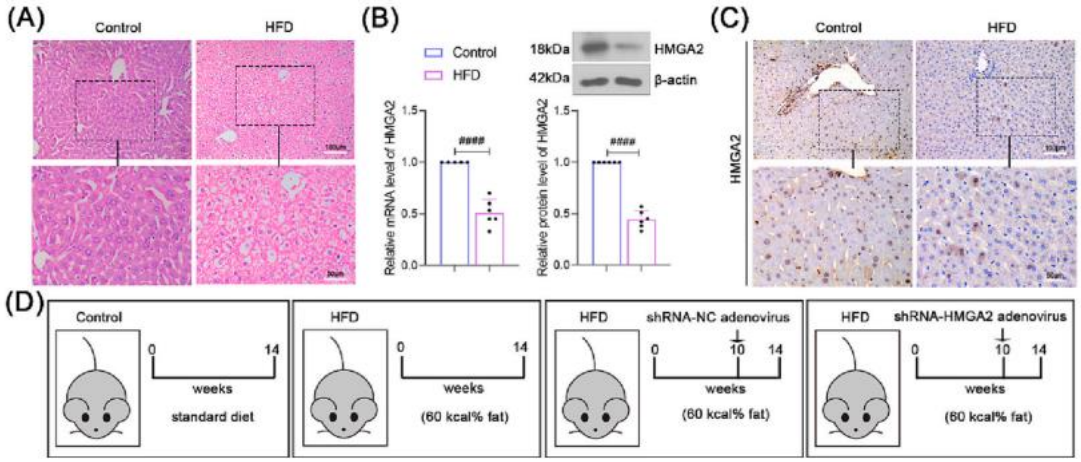

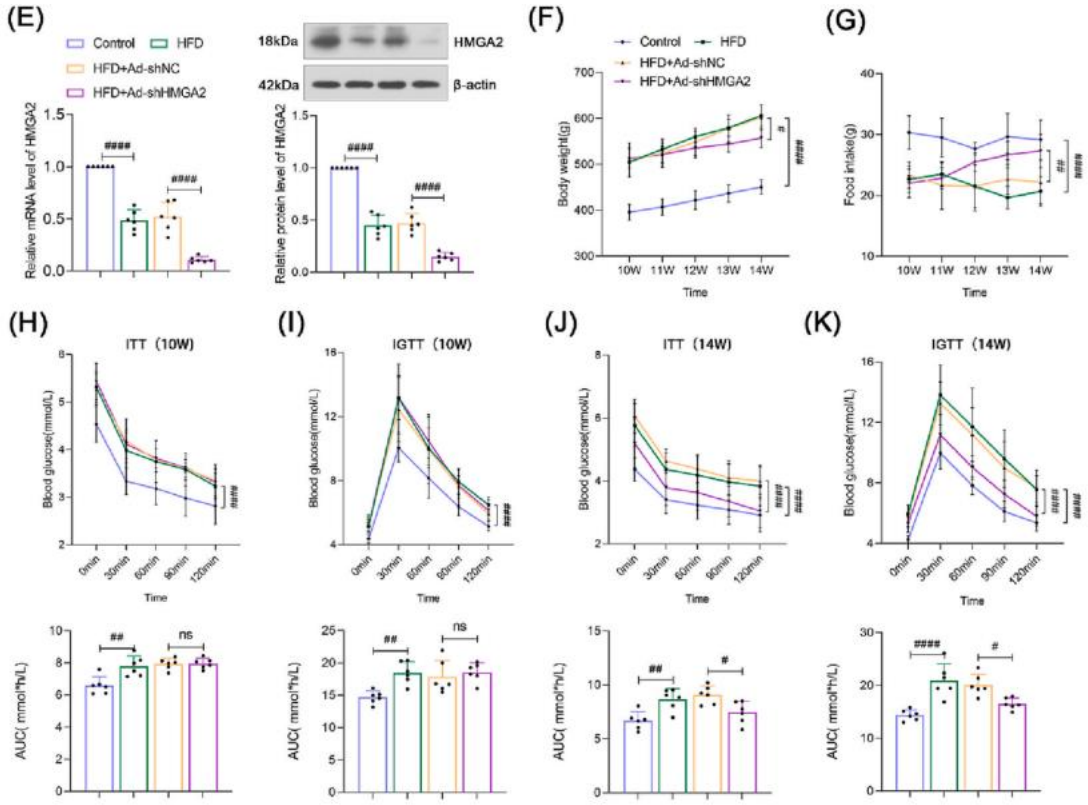

Fig. 2. HMGA2 knockdown improved insulin sensitivity in NAFLD rats. (A) H&E staining showed the pathological changes of rat liver tissues after high-fat diet (the scale bar represented 100 μm and 50 μm). (B) The mRNA and protein levels of HMGA2 were determined by real-time PCR and western blot. (C) HMGA2 expression was detected by immunohistochemistry staining (the scale bar represented 100 μm and 50 μm). (D) An adenoviral vector carrying shRNA targeting HMGA2 in HFD rats was established. (E) The knockdown efficiency of HMGA2 was detected by real-time PCR and western blot. (F) and (G) Body weight and food intake of rats were detected at 10 to 14 weeks. (H–K) In ITT and IGTT experiments, blood glucose levels and AUC were determined at 10th and 14th week. (#, $p < 0.05$; ##, $p < 0.01$; ####, $p < 0.0001$ vs. control or HFD + Ad-shNC).

3.3. HMGA2 knockdown relieved liver injury in NAFLD rats

To verify the function of HMGA2 knockdown on liver injury in NAFLD rats, the liver index was measured, we found considerable decrease in liver index in the HMGA2 knockdown group compared to the negative control (Fig. 3A). Notably, liver injury was substantially quantified by circulating liver enzymes AST and ALT activities in serum, we observed that HMGA2 knockdown restrained HFD-mediated liver function impairment (Fig. 3B-C). In particular, to ascertain the response of liver structure to HFD stress, we assessed the degree of liver injury using histological analysis. As determined by H&E staining, the liver tissues of the HFD group exhibited more robust liver cell cord derangement, intercellular spaces dilatation and inflammatory cell infiltration, while the control rats showed normal lobular architecture with central veins and radiating hepatic cords, confirming that HFD-fed rats developed definite NAFLD. As expected, these changes were efficiently alleviated due to HMGA2 knockdown (Fig. 3D). Moreover, steatosis, hepatocyte ballooning and inflammation were assessed and scores were given (Table 2). The individual scores were added together to produce the overall NAFLD activity score (NAS). Interestingly, NAS results displayed that the total scores of steatosis, lobular multifocal portal inflammation and hepatocyte ballooning in NAFLD rats treated with HMGA2 knockdown were the lowest, as compared with controls (Fig. 3E).

In short, we conclude that decreasing HMGA2 repairs rat liver injury induced by HFD.

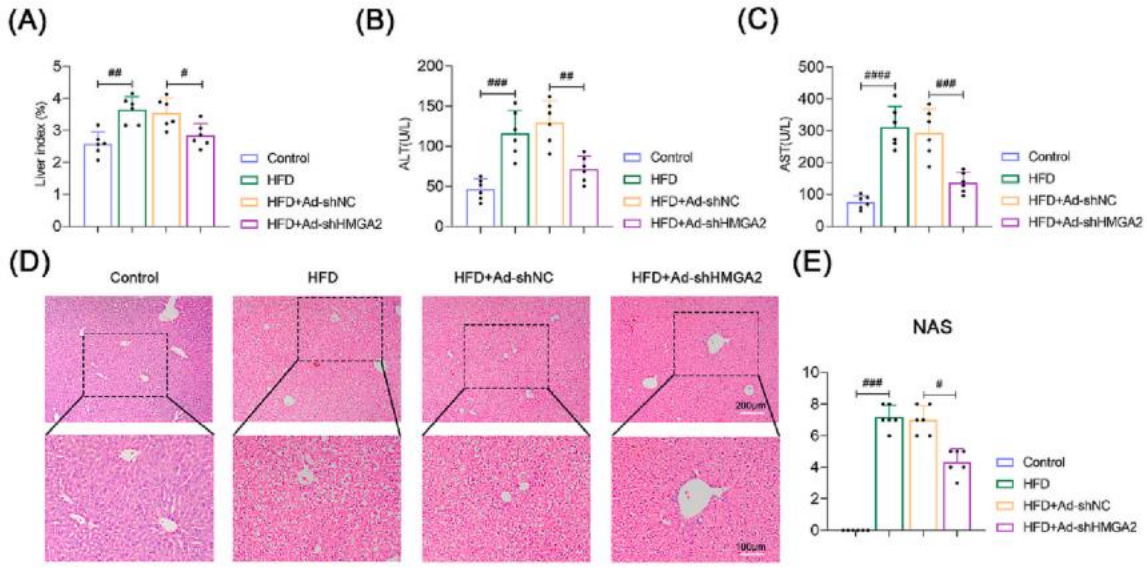

Fig. 3. HMGA2 knockdown relieved liver injury in NAFLD rats. (A) Liver index (liver index = liver wet weight/body weight×100%). (B) and (C) ALT and AST activities in serum. (D) and (E) H&E staining and NAS showed the degree of liver tissue damage after HMGA2 knockdown (the scale bars represented 200 μm and 100 μm). (#, $p < 0.05$; ##, $p < 0.01$; ###, $p < 0.001$; ####, $p < 0.0001$ vs. control or HFD + Ad-shNC).

3.4. HMGA2 knockdown reduced liver lipid deposition in NAFLD rats

We also concentrated on the efficacy of HMGA2 in liver lipid deposition in NAFLD rats. Based on gross observation and quantitative analysis of Oil Red O staining, the HFD group presented very high liver lipid content, while HMGA2 knockdown markedly reduced HFDinduced lipid accumulation compared with the negative control (Fig. 4A). Furthermore, we observed that HFD treatment increased the TC and TG levels, while HMGA2 knockdown resulted in a pronounced decline in TC and TG levels both in serum and liver tissues (Fig. 4B-E). In addition, results of real-time PCR and western blot further demonstrated that the expression levels of the CD36 (a fatty acid transporter) and fatty acid synthase (FAS, a fatty acid synthesis-related enzyme) were also significantly downregulated in liver tissues of HMGA2 knockdowntreated NAFLD rats (Fig. 4F-H). Collectively, these data support a vital role of HMGA2 knockdown in reducing HFD-induced lipid deposition, implying that downregulation of HMGA2 is an efficient approach to prevent progressive lipid accumulation.

Table 2
Grading NAFLD activity score (NAS) [23,24].

Steatosis	Hepatocyte ballooning	Lobular inflammation	NAS
<5% (0)	None (0)	None (0)	0
5–33% (1)	Rare or few (1)	1–2 foci/20 × field (1)	3
34–66% (2)	Many (2)	2–4 foci/20 × field (2)	6
>66% (3)	Many (2)	>4 foci/20 × field (3)	8

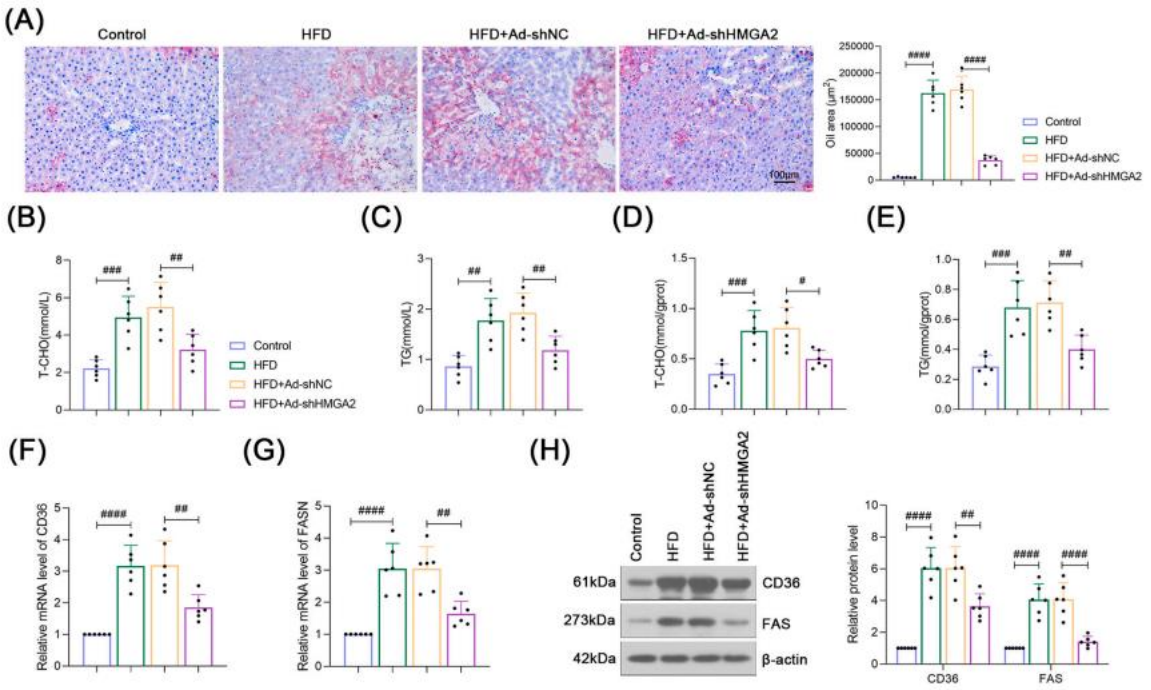

Fig. 4. HMGA2 knockdown reduced liver lipid deposition in NAFLD rats. (A) The effect of HMGA2 knockdown on lipid deposition was measured by Oil Red O staining in liver tissues (the scale bar represented 100 μm). (B) and (D) Total cholesterol (TC) levels in serum and liver tissues. (C) and (E) Triglyceride (TG) levels in serum and liver tissues. (F–H) The mRNA and protein levels of CD36 and FAS. (#, $p < 0.05$; ##, $p < 0.01$; ###, $p < 0.001$; ####, $p < 0.0001$ vs. control or HFD + Ad-shNC). (For interpretation of the references to colour in this figure legend, the reader is referred to the web version of this article.)

3.5. HMGA2 knockdown restrained liver inflammation in NAFLD rats

Next, to investigate the impact of HMGA2 on liver inflammation in NAFLD rats, we determined the mRNA and protein levels of related proinflammatory cytokines by real-time PCR and ELISA. These data certified that the levels of TNF-α, IL-6, IL-1β and MCP-1 were all elevated in HFD-fed rats, while significantly reduced in the HMGA2 knockdown treated NAFLD rats, indicating that HMGA2 knockdown inhibited the production of these inflammatory cytokines (Fig. 5A-D). Thus, we speculated that HMGA2 knockdown may play an anti-inflammatory role. Accordingly, this hypothesis was further verified with the protein expression of CD68 (a sign of potential inflammatory infiltration), as indicated by immunofluorescence staining (Fig. 5E).

In conclusion, these results suggest that reduction in HMGA2 expression presents significant anti-inflammatory effects in the progression of NAFLD.

3.6. HMGA2 knockdown attenuated liver fibrosis in NAFLD rats

Considering that chronic HFD treatment can cause fibrosis [25]. Functionally, to further analyze the potential benefit of HMGA2 in liver fibrosis in NAFLD rats, we firstly applied Masson staining and Fibrosis Grading to detect the degree of liver fibrosis. The results displayed that the severe steatosis with fibrosis in the HFD-fed rats evidently verified the progression from NAFLD to NASH. However, compared with the negative control-treated rats, less liver fibrosis was observed in the HMGA2 knockdown group, as determined by the number of fibrotic areas in the liver sections (Fig. 6A). These results were further confirmed in Fibrosis Grading (Table 3), suggesting that HMGA2 knockdown negated this phenotypic alteration and further protected rats from HFDmediated liver fibrosis (Fig. 6A). We also obtained the same results by Sirius Red staining (Fig. 6B). Besides, as demonstrated by immunohistochemical staining, the abundance of fibrous proteins α-SMA and Collagen I were

certainly increased in answer to HFD treatment, and these parameters were suppressed by HMGA2 knockdown (Fig. 6C). Moreover, western blot results proved that HMGA2 knockdown decreased the protein levels of the profibrotic factor TGF-β1 and the phosphorylation of SMAD2/3, with no difference in SMAD2/3 levels (Fig. 6D), thus inhibiting the activation of TGF-β1/SMAD signaling pathway.

Totally, the above results certify that knockdown of HMGA2 exhibits a strong inhibitory potential in severe liver fibrosis of NAFLD rats.

3.7. HMGA2 knockdown relieved PA-induced hepatocyte injury in HepG2 cells

Given the potential role of HMGA2 was identified in vivo, we extended the function of HMGA2 on PA-induced hepatocyte injury in HepG2 cells. Firstly, we used siRNA-HMGA2 to decrease its expression and examined the knockdown effect of HMGA2 using real-time PCR and western blot analyses in HepG2 cells (Fig. 7A). Then transfected cells were treated with 400 μmol/l palmitic acid (PA) for 24 h to cause hepatocyte injury for subsequent experiments. Although accumulation was achieved in PA-treated cells, these changes were attenuated by HMGA2 knockdown, as illustrated by Oil Red O staining (Fig. 7B). In addition, TC, TG levels as well as CD36 and FAS protein levels were obviously downregulated in HMGA2-silenced cells (Fig. 7CE). Likewise, at the molecular levels, quantitative analyses suggested that HMGA2 knockdown markedly decreased the mRNA levels of TNF-α, IL-6, IL-1β and MCP-1 relative to the negative control (Fig. 7F-I). The results were further identified at the protein levels using ELISA (Fig. 7FI).

Similar to in vivo data, we further identify that knockdown of HMGA2 relieves PA-induced hepatocyte injury, thereby delaying the progression of NAFLD.

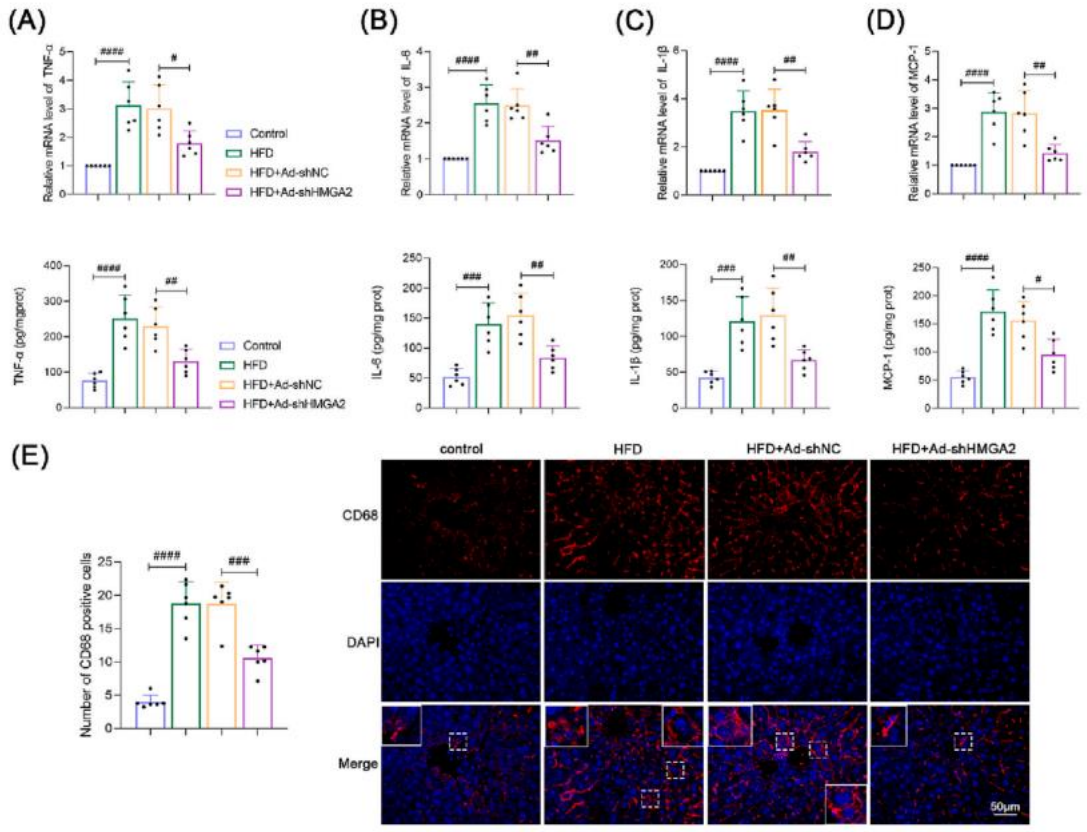

Fig. 5.
HMGA2 knockdown restrained liver inflammation in NAFLD rats. (A-D) The levels of TNF-α, IL-6, IL-1β and MCP-1 were determined by real-time PCR and ELISA. (E) CD68 expression was identified by immunofluorescent staining (the rectangles indicated infiltration of CD68 and the scale bar represented 50 μm). (#, $p < 0.05$; ##, $p < 0.01$; ###, $p < 0.001$; ####, $p < 0.0001$ vs. control or HFD + Ad-shNC).

3.8. HMGA2 knockdown attenuated TGF-β1-induced liver fibrosis in hepatic stellate cells

As displayed previously, HMGA2 knockdown protected NAFLD rats against the development of liver fibrosis in vivo, we also assumed that knockdown of HMGA2 played a significant role in aggressive liver fibrosis induced by TGF-β1 administration in vitro. To test this speculation, LX-2 cells were transfected with siRNA-HMGA2, and results of real-time PCR and western blot suggested that siRNA-induced HMGA2 knockdown potently inhibited its expression in TGF-β1-induced hepatic stellate cells (Fig. 8A). With respect to fibrosis, infected cells were treated with 10 ng/ml TGF-β1 for 24 h and collected for the following experiments. As observed, immunofluorescence staining results confirmed that the expression of α-SMA was significantly reduced in HMGA2-silenced cells (Fig. 8B). In agreement with the staining analysis, western blot results further revealed that HMGA2 knockdown obviously declined the protein levels of fibrous proteins α-SMA and Collagen I, as well as the phosphorylation of SMAD2/3, respectively, though with no significant effect on SMAD2/3 levels (Fig. 8C).

In sum, the above data corroborate that knocking-down HMGA2 also inhibits the activation of TGF-β1/SMAD signaling pathway and attenuates TGF-β1-induced liver fibrosis in hepatic stellate cells, consistent with the in vivo studies.

3.9. SNAI2 overexpression blocked the inhibitory effect of HMGA2 knockdown on hepatocyte injury

Strikingly, HMGA2 knockdown led to downregulation of SNAI2 levels, at both mRNA and protein levels in vivo and in vitro (Fig. 9A-B). Thus, we wondered whether HMGA2 regulated the transcription of SNAI2. According to the analysis data from Human TFDB, there may be binding sites on the promoter region of SNAI2. Based on luciferase reporter gene assays, interestingly, we observed that HMGA2 over expression significantly increased the luciferase activity, indicating that HMGA2 activated the transcription of SNAI2 (Fig. 9C-D)

To further elucidate the relationship between HMGA2 and SNAI2, a SNAI2 overexpression was constructed to rescue the function of HMGA2 knockdown. Firstly, SNAI2 was detected by real-time PCR and western blot in both HepG2 and LX-2 cells transfected with SNAI2 overexpressed (Fig. 9E/M). After SNAI2 overexpression plasmid was co-transfected with siRNA-HMGA2, we applied Oil Red O staining to detect intracellular lipid droplet formation. Knocking-down HMGA2 inhibited the lipid accumulation in PA-treated HepG2 cells, which was abolished by SNAI2 overexpression (Fig. 9F). By comparison, TC and TG levels as well as CD36 and FAS protein levels were also downregulated in HMGA2 silenced-cells, and these factors levels were upregulated by SNAI2 overexpression (Fig. 9G-H). In addition, real-time PCR results further revealed that the mRNA levels of TNF-α, IL-6, IL-1β and MCP-1, which were declined by HMGA2 knockdown, were elevated with SNAI2overexpression and HMGA2 knockdown treatment (Fig. 9I-L). On the other hand, western blot results demonstrated that compared to the effects of HMGA2 knockdown, SNAI2 overexpression obviously upregulated the protein levels of fibrous proteins α-SMA and Collagen I in TGF-β1-treated LX-2 cells (Fig. 9N). On the basis of these findings, we investigate that HMGA2 activates the transcription of SNAI2. More importantly, exogenous upregulation of SNAI2 effectively blocks the inhibitory effect of HMGA2 knockdown on hepatocyte injury in vitro, suggesting that SNAI2 is necessary for the function of HMGA2 in NAFLD progression (Fig. 10).

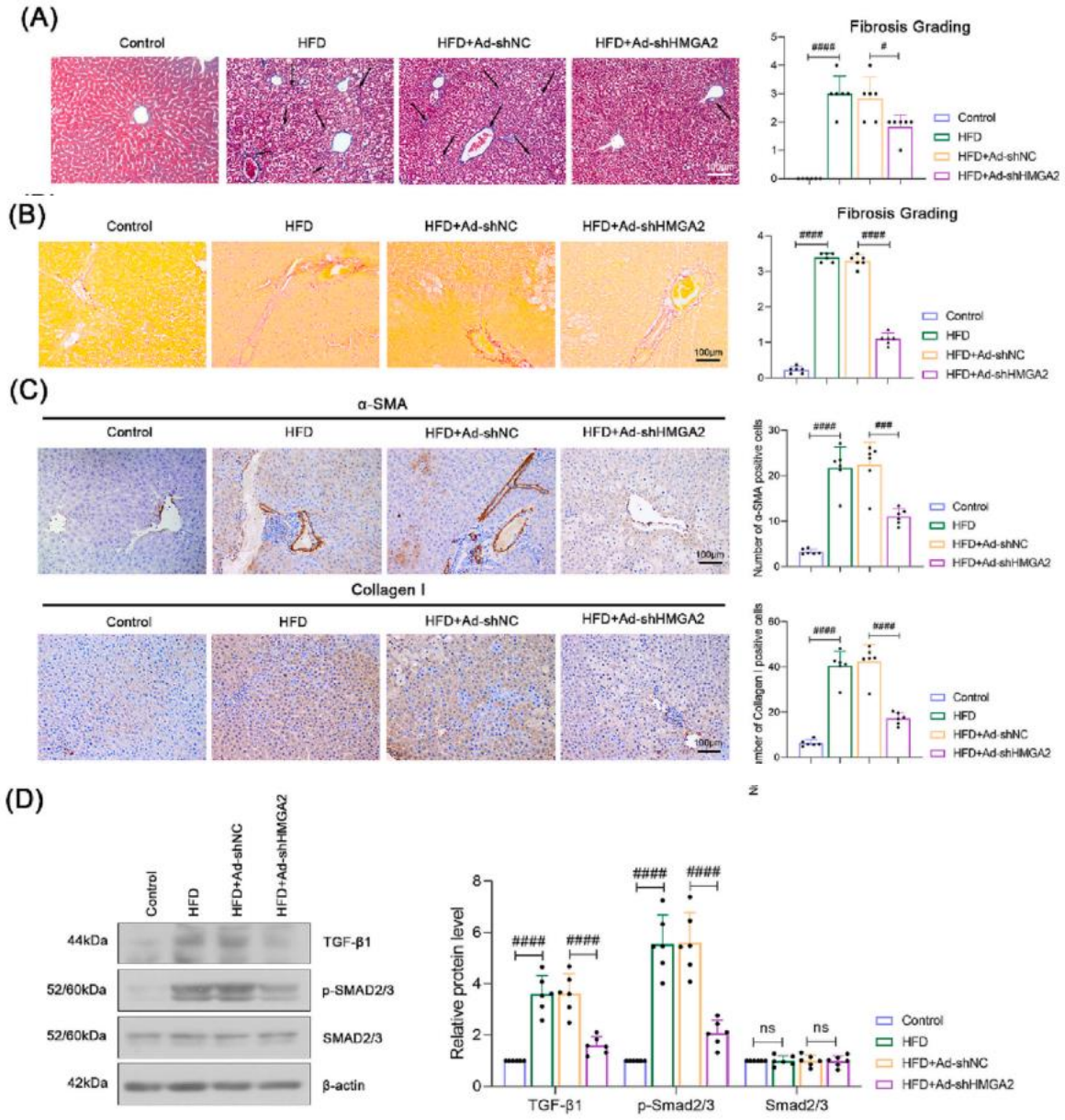

Fig. 6. HMGA2 knockdown attenuated liver fibrosis in NAFLD rats. (A) Masson staining and Fibrosis Grading were applied to detect the degree of liver fibrosis (the arrows indicated fibrosis and the scale bar represented 100 μm). (B) Sirius Red staining was also used to examine the liver fibrosis (the scale bar represented 100 μm). (C) Expression of α-SMA and Collagen I were detected by immunohistochemistry staining (the scale bar represented 100 μm). (D) The protein levels of TGF-β1 and SMAD2/3, and the phosphorylation of SMAD2/3. (#, $p < 0.05$; ###, $p < 0.001$; ####, $p < 0.0001$ vs. control or HFD + Ad-shNC). (For interpretation of the references to colour in this figure legend, the reader is referred to the web version of this article.)

Table 3
Grading Fibrosis [23].

Definition	Score
None	0
Perisinusoidal or periportal	1
Perisinusoidal and portal/periportal	2
Bridging fibrosis	3
Cirrhosis	4

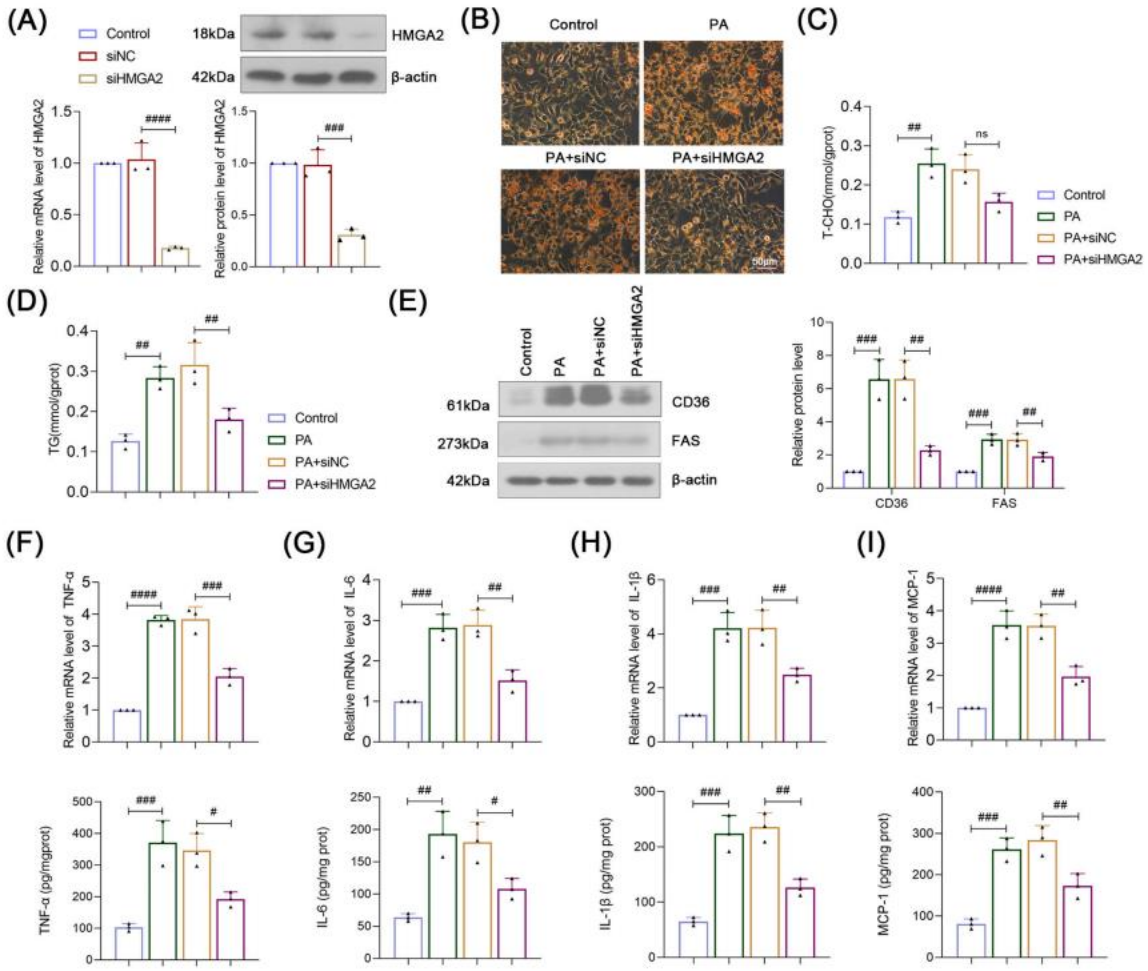

Fig. 7. HMGA2 knockdown relieved PA-induced hepatocyte injury in HepG2 cells. (A) The knockdown efficiency of HMGA2 was detected in HepG2 cells by realtime PCR and western blot. (B) Oil red O staining was used to detect intracellular lipid droplet formation (the scale bar represented 50 μm). (C) and (D) TC and TG levels in HepG2 cells. (E) The protein levels of CD36 and FAS. (F–I) The mRNA and protein levels of TNF-α, IL-6, IL-1β and MCP-1. (#, $p < 0.05$; ##, $p < 0.01$; ###, $p < 0.001$; ####, $p < 0.0001$ vs. control or PA + siNC). (For interpretation of the references to colour in this figure legend, the reader is referred to the web version of this article.)

Fig. 8. HMGA2 knockdown attenuated liver fibrosis in TGF-β1-induced hepatic stellate cells. (A) The knockdown efficiency of HMGA2 was detected in LX-2 cells by real-time PCR and western blot. (B) α-SMA expression was identified by immunofluorescent staining (the arrow indicated α-SMA expression and the scale bar represented 50 μm). (C) The protein levels of α-SMA, Collagen I and SMAD2/3, and the phosphorylation of SMAD2/3. (##, $p < 0.01$; ###, $p < 0.001$; ####, $p < 0.0001$ vs.

TGF-β1 + siNC).

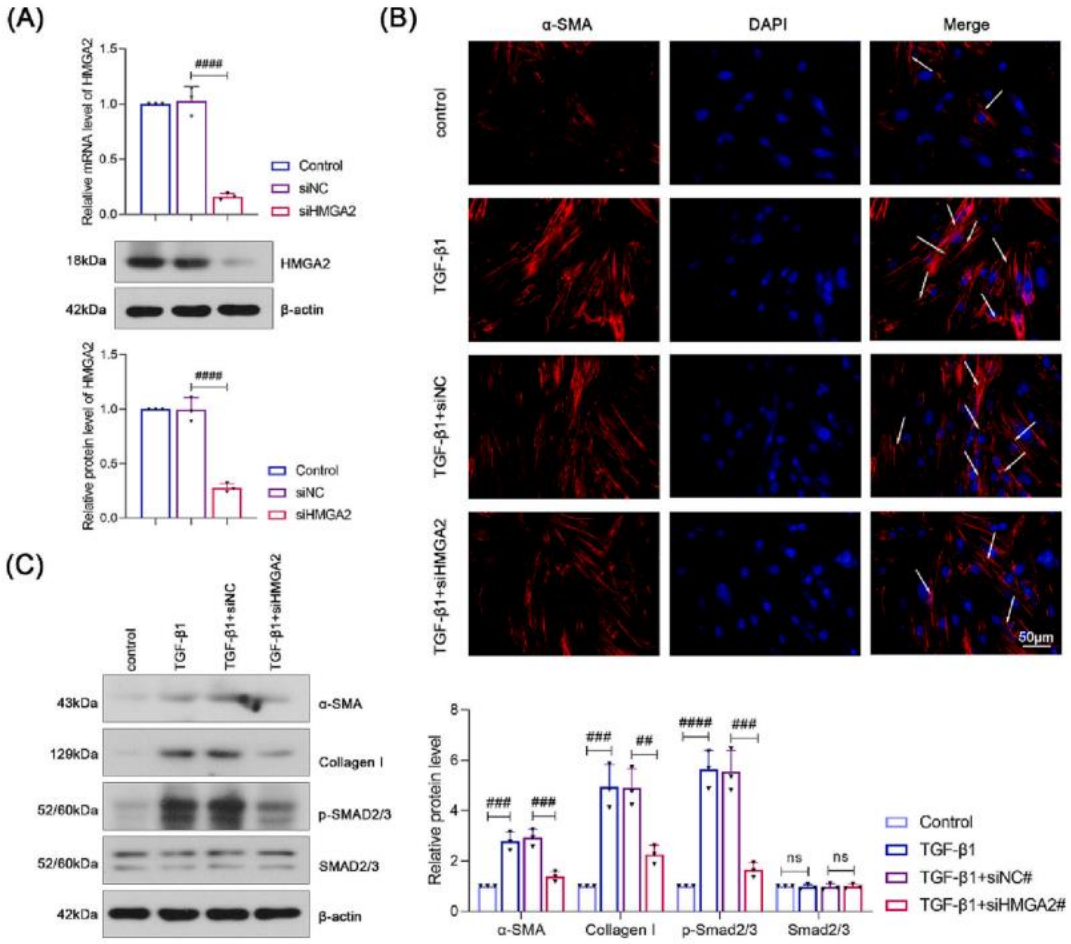

Fig. 8. HMGA2 knockdown attenuated liver fibrosis in TGF-β1-induced hepatic stellate cells. (A) The knockdown efficiency of HMGA2 was detected in LX-2 cells by real-time PCR and western blot. (B) α-SMA expression was identified by immunofluorescent staining (the arrow indicated α-SMA expression and the scale bar represented 50 μm). (C) The protein levels of α-SMA, Collagen I and SMAD2/3, and the phosphorylation of SMAD2/3. (##, $p < 0.01$; ###, $p < 0.001$; ####, $p < 0.0001$ vs. TGF-β1 + siNC).

4. Discussion

Previous studies have suggested that feeding rats with a high-fat diet induces hepatic steatosis and liver damage, which are characteristics of NAFLD, providing a suitable model for this disease [26,27]. In this study, a high-fat diet model induced NAFLD was successfully established to explore the pathogenesis of NAFLD. HMGA2 is a multifunctional regulator involved in development, differentiation, stemness, tumorigenesis and fibrogenesis [28]. However, its role in NAFLD has not been identified. Our results presented that HMGA2 expression was decreased in liver tissues of NAFLD rats, consistent with the results of the GEO database. In the present study, we knocked down HMGA2 in animal and cellular models, which may play a protective role. Then, we investigated the multiple roles of HMGA2 knockdown in the development of NAFLD in vivo and in vitro. Numerous studies have reported that the highest prevalence of NAFLD is found in populations with obesity or type 2 diabetes [29,30]. Obesity and its metabolic consequences are regarded the major contributors to fat accumulation [31]. Moreover, impaired insulin sensitivity leads to type 2 diabetes [32]. Markowski et al. proved that HMGA2 was significantly elevated in patients with obesity and type 2 diabetes [33]. Additionally, HMGA2-deficient mice were resistant to dietinduced obesity [34,35 studies, our study revealed that after 14 weeks of feeding, HMGA2 knockdown decreased body weight and increased food intake. This may be due to HFD feeding, which led to abnormal food

intake of HFD rats, while decreasing HMGA2 alleviated this situation and restored food intake to normal level. Furthermore, HMGA2 knockdown improved insulin sensitivity by downregulating blood glucose levels to normal levels in NAFLD rats, indicating that knocking-down HMGA2 exhibited a significant inhibition of obesity and type 2 diabetes.

NAFLD causes many types of liver injury, and its histological features include steatosis, inflammation and hepatocyte ballooning [23,36]. In this study, we found that HMGA2 knockdown largely decreased liver index, suggesting that the liver injury of the rats treated with shRNAHMGA2 was improved. Also, it is well known that ALT and AST are used as indicators of liver index, reflecting the degree of liver injury [37]. We further verified that HMGA2 knockdown obviously inhibited circulating liver enzymes ALT and AST activities in serum. More importantly, results of histological analysis and NAS indicated that HMGA2 knockdown reduced steatosis, lobular multifocal portal inflammation and hepatocyte ballooning. Overall, we validated the role of HMGA2 knockdown in restoring HFD-induced liver injury.

The earliest stage of NAFLD is caused by excessive lipid accumulation in the liver because of an increased delivery of fatty acids from adipose tissue accompanied by an imbalance between lipid degradation and de novo lipid synthesis [38,39]. De novo synthesis of lipids in the liver is a common targeted pathway to suppress lipid production [40]. FAS as a key metabolic multi-enzyme is responsible for the terminal catalytic step in fatty acid synthesis [41]. CD36 belongs to Class B scavenger receptor family and participates in fatty acid uptake [42]. Xi et al. suggested that HMGA2 was implicated in adipose tissue development [8]. Moreover, downregulation of HMGA2 suppressed adipogenesis of human adipose-derived mesenchymal stem cells [43]. Thus, it is necessary to investigate the efficacy of HMGA2 in lipid deposition. Herein, our analysis demonstrated that HMGA2 knockdown evidently reduced lipid accumulation, TC and TG levels and the expression levels of these two metabolic enzymes in NAFLD rats, respectively, confirming that knockdown of HMGA2 played a key role in the earliest stage of NAFLD and further led to decelerate the development of NAFLD.

It is suggested that the liver is an important immune organ, exerting a key role in immune regulation, especially its immune cells and secreted cytokines that are related to abnormal metabolism. These cells and cytokines modulate the local and systemic inflammation response in the liver [44]. Inflammatory response is closely related to the occurrence, development and prognosis of cancer, and can be activated by increasing the expression of pro-inflammatory cytokines such as TNF-α, IL-6 and IL-1β [45,46]. Accumulation of lipids triggers a chronic inflammatory response [39,47]. When TG levels in hepatocytes rise, the production of toxic free radicals (such as RNS and ROS) activates necrotic pathways and directly increases the levels of pro-inflammatory cytokines, including TGF-β, causing damage to hepatocytes [48]. Additionally, CD68 is considered as a valuable cytochemical marker in histochemical analysis of inflammatory tissues and other immunohistopathological applications [49]. In recent years, various studies have proven that HMGA2 promotes inflammatory response by enhancing the expression of pro-inflammatory cytokines [50,51]. Thus, blocking the expression of inflammatory factors in adipose tissue to prevent inflammatory response is a common method. Here, our study also identified that HMGA2 knockdown restrained liver inflammation in NAFLD rats with a concomitant reduction in the expression of these proinflammatory cytokines and CD68, which may contribute to antiinflammatory effects in the progression of NAFLD. Deeply, these inflammatory cytokines (TNF-α, IL-6 and others) have been reported to promote insulin resistance [52], which was in line with our previous studies that HMGA2 knockdown relived insulin resistance and further improved insulin sensitivity in NAFLD rats. Likewise, in vitro results showed that HMGA2 knockdown reduced the accumulation of lipids and downregulated the expression of pro-inflammatory genes in HepG2 cells, thereby relieving PA-induced hepatocyte injury.

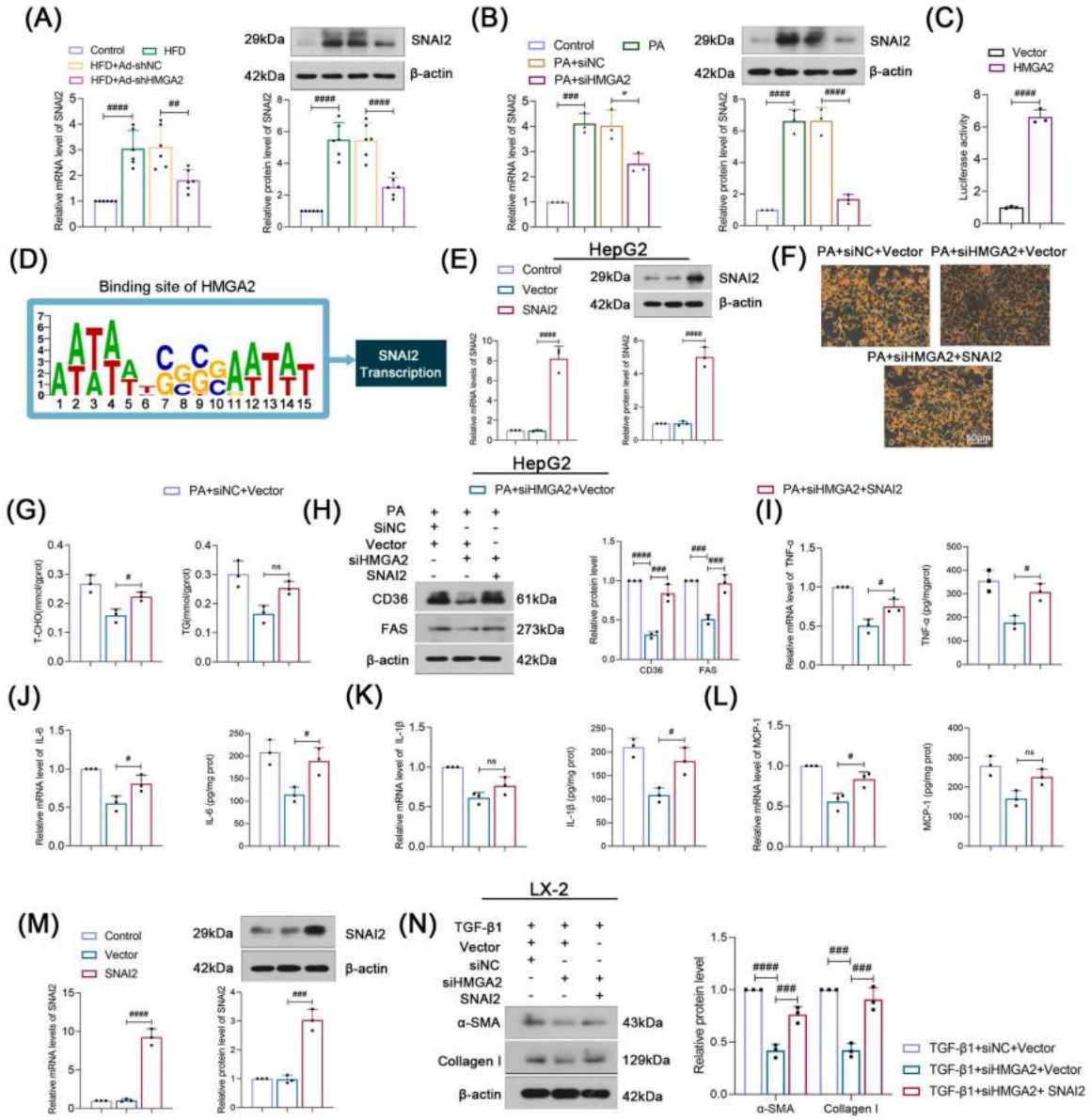

Fig. 9. SNAI2 overexpression blocked the inhibitory effect of HMGA2 knockdown on hepatocyte injury. (A-B) The mRNA and protein levels of SNAI2 after HMGA2 knockdown both in vivo and in vitro (##, $p < 0.01$; ####, $p < 0.0001$ vs. control or HFD + Ad-shNC; #, $p < 0.05$; ###, $p < 0.001$; ####, $p < 0.0001$ vs. control or PA + siNC). (C–D) The SNAI2 promoter construct was co-transfected with HMGA2 overexpression plasmid or vector plasmid, and the relative luciferase activity was determined. (####, $p < 0.0001$ vs. vector+pGL3-SNAI2 promoter) Graphical representation of predicted HMGA2 binding site in the SNAI2 promoter region. (E) The mRNA and protein levels of SNAI2 overexpression were determined by real-time PCR and western blot in HepG2 cells. (####, $p < 0.0001$ vs. vector). Then SNAI2 overexpression plasmid was co-transfected with siHMGA2 or vector. (F) Oil red O staining was used to detect intracellular lipid droplet formation in PA-induced HepG2 cells (the scale bar represented 50 μm). (G) TC and TG levels. (H) The protein levels of CD36 and FAS (###, $p < 0.001$; ####, $p < 0.0001$ vs. PA + siHMGA2 + Vector). (I-L) The mRNA levels of TNF-α, IL-6, IL-1β and MCP-1. (#, $p < 0.05$ vs. PA + siHMGA2 + Vector). (M) The mRNA and protein levels of SNAI2 overexpression were determined by real-time PCR and western blot in LX-2 cells. (###, $p < 0.001$; ####, $p < 0.0001$ vs. vector). (N) The protein levels of α-SMA and Collagen I in TGF-β1-treated LX-2 cells (###, $p < 0.001$; ####, $p < 0.0001$ vs. TGF-β1 + siHMGA2 + Vector). (For interpretation of the references to colour in this figure legend, the reader is referred to the web version of this article.)

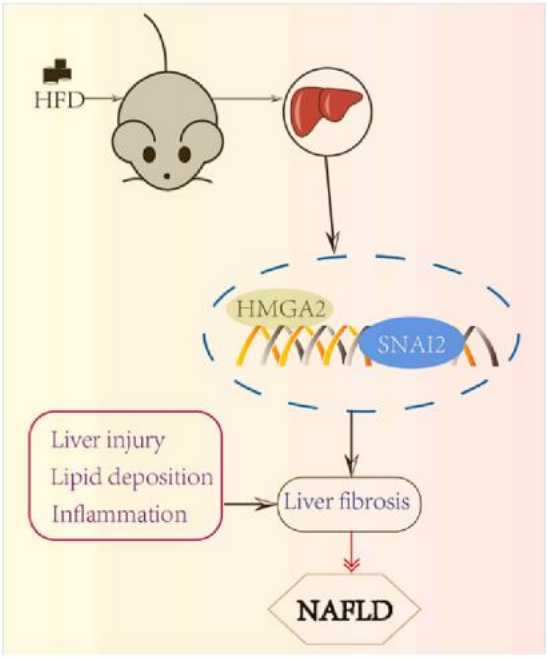

Fig. 10. A scheme of HMGA2 role in NAFLD. HMGA2 induces the transcription of SNAI2 to trigger the process of NAFLD.

Liver fibrosis is characteristic of progression from NAFL to NASH [53]. EMT exerts a vital role in cellular differentiation during embryonic development, tumor invasion and tissue fibrosis [54]. TGF-β1, an important profibrogenic cytokine, which accelerates fibrosis and is a crucial inducer of EMT [55,56]. The pleiotropy of TGF-β plays a role in almost every stage of liver disease progression, from simple lipid accumulation to hepatic carcinomas, but is more pronounced in fibrosis and cirrhosis [57]. Besides, the complex interaction between inflammatory stress and lipid accumulation, assisted by mediators such as proinflammatory interleukins and TGF-β1, forms the basis for the progression of NAFLD [58,59]. When TGF-β receptors are activated, it can directly bind to SMADs and their phosphorylated products, and further activate TGF-β1/SMAD signaling pathway by increasing the nuclear translocation of p-SMAD2/3 to stimulate the expression of downstream substrates, which may lead to liver fibrosis [60]. Moreover, activation of TGF-β1/SMAD signaling pathway leads to excessive deposition of fibrosis-related proteins, such as α-SMA and collagen I [61,62]. Notably, previous studies have claimed that HMGA2 is an important regulator of EMT and involved in the process of some fibrotic diseases [9,63]. For example, HMGA2 knockdown reduced cellular fibrosis levels in human hepatic stellate cells [9]. Additionally, HMGA2 overexpression promoted high glucose-induced fibrosis in human glomerular mesangial cells [64]. In this study, we identified that HMGA2 knockdown downregulated the expression of fibrous proteins α-SMA and Collagen I. Also, HMGA2 knockdown decreased the protein expression levels of TGF-β1 and the phosphorylation of SMAD2/3, thus inhibiting the activation of TGF-β1/SMAD signaling pathway in vivo and in vitro. The above data presented confirmed that HMGA2 knockdown exerted the beneficial anti-fibrotic functions. Thus, our analysis implied that knockdown of HMGA2 showed obvious effects on all stages of NAFLD and the application of shRNA or siRNA to reduce HMGA2 expression in the liver might be a feasible strategy for the treatment of NAFLD.

Transcription factor SNAI2 is an evolutionarily conserved C2H2 zinc finger protein that coordinates biological processes critical for tissue development and tumorigenesis [20]. SNAI2 was initially considered as a EMT transcription factor and participated in a range of biological processes, including tumor metastasis, cellular differentiation, vascular remodeling and DNA damage repair [65]. Specifically, Slab´ akova ´ E et al. has revealed that SNAI2 is vital for TGF-β1-induced EMT [66]. In this

study, we confirmed that HMGA2 knockdown significantly downregulated the expression of SNAI2. Importantly, previous studies have demonstrated that HMGA2 is recruited to binding sites on the SNAI2 promoter and directly facilitates the transcription of SNAI2 [18,22]. Moreover, HMGA2 directly regulated the expression of SNAI2 to promote the malignant progression of head and neck squamous cell carcinoma and acquire the characteristics of tumor stem cells [18]. In addition, HMGA2 induced SNAI2 expression to trigger EMT and contribute to the progression of colon cancer [22]. In accordance with the current study, we discovered that HMGA2 activated SNAI2 transcription and SNAI2 overexpression efficiently blocked the inhibitory effect of HMGA2 knockdown on hepatocyte injury in vitro, implying that SNAI2 affected the role of HMGA2 knockdown in NAFLD progression.

Altogether, we systematically dissect that knockdown of HMGA2 exhibits excellent alleviating effects on the process of NAFLD. In addition, SNAI2 has been demonstrated to be indispensable for the function of HMGA2 in NAFLD progression (Fig. 10). These findings indicate that inhibition of HMGA2 may be very valuable for future clinical application.

References

[1] E.K. Spengler, R. Loomba, Recommendations for diagnosis, referral for liver biopsy, and treatment of nonalcoholic fatty liver disease and nonalcoholic steatohepatitis, Mayo Clin. Proc. 90 (9) (2015) 1233–1246.

[2] C.D. Williams, J. Stengel, M.I. Asike, D.M. Torres, J. Shaw, M. Contreras, C. L. Landt, S.A. Harrison, Prevalence of nonalcoholic fatty liver disease and nonalcoholic steatohepatitis among a largely middle-aged population utilizing ultrasound and liver biopsy: a prospective study, Gastroenterology 140 (1) (2011) 124–131.

[3] E.M. Brunt, V.W. Wong, V. Nobili, C.P. Day, S. Sookoian, J.J. Maher, E. Bugianesi, C.B. Sirlin, B.A. Neuschwander-Tetri, M.E. Rinella, Nonalcoholic fatty liver disease, Nat Rev Dis Primers 1 (2015) 15080.

[4] M.M. Yeh, E.M. Brunt, Pathological features of fatty liver disease, Gastroenterology 147 (4) (2014) 754–764.

[5] Y. Takahashi, K. Sugimoto, H. Inui, T. Fukusato, Current pharmacological therapies for nonalcoholic fatty liver disease/nonalcoholic steatohepatitis, World J. Gastroenterol. 21 (13) (2015) 3777–3785.

[6] H. Tilg, A.R. Moschen, Evolution of inflammation in nonalcoholic fatty liver disease: the multiple parallel hits hypothesis, Hepatology 52 (5) (2010) 1836–1846.

[7] J. Wu, Z. Liu, C. Shao, Y. Gong, E. Hernando, P. Lee, M. Narita, W. Muller, J. Liu, J. J. Wei, HMGA2 overexpression-induced ovarian surface epithelial transformation is mediated through regulation of EMT genes, Cancer Res. 71 (2) (2011) 349–359.

[8] Y. Xi, W. Shen, L. Ma, M. Zhao, J. Zheng, S. Bu, S. Hino, M. Nakao, HMGA2 promotes adipogenesis by activating C/EBPbeta-mediated expression of PPARgamma, Biochem. Biophys. Res. Commun. 472 (4) (2016) 617–623.

[9] K. McDaniel, L. Huang, K. Sato, N. Wu, T. Annable, T. Zhou, S. Ramos-Lorenzo, Y. Wan, Q. Huang, H. Francis, S. Glaser, H. Tsukamoto, G. Alpini, F. Meng, The let- 7/Lin28 axis regulates activation of hepatic stellate cells in alcoholic liver injury, J. Biol. Chem. 292 (27) (2017) 11336–11347.

[10] D. Rong, F. Wu, C. Lu, G. Sun, X. Shi, X. Chen, Y. Dai, W. Zhong, X. Hao, J. Zhou, Y. Xia, W. Tang, X. Wang, m6A modification of circHPS5 and hepatocellular carcinoma progression through HMGA2 expression, Mol. Ther. Nucleic Acids 26 (2021) 637–648.

[11] A. Mahajan, Z. Liu, L. Gellert, X. Zou, G. Yang, P. Lee, X. Yang, J.J. Wei, HMGA2: a biomarker significantly overexpressed in high-grade ovarian serous carcinoma, Mod. Pathol. 23 (5) (2010) 673–681.

[12] H. Huang, H. Li, X. Chen, Y. Yang, X. Li, W. Li, C. Huang, X. Meng, L. Zhang, J. Li, HMGA2, a driver of inflammation, is associated with hypermethylation in acute liver injury, Toxicol. Appl. Pharmacol. 328 (2017) 34–45.

[13] L.M. Resar, The high mobility group A1 gene: transforming inflammatory signals into cancer? Cancer Res. 70 (2) (2010) 436–439.

[14] A. Tesfaye, F. Di Cello, J. Hillion, B.M. Ronnett, O. Elbahloul, R. Ashfaq, S. Dhara, E. Prochownik, K. Tworkoski, R. Reeves, R. Roden, L.H. Ellenson, D.L. Huso, L. M. Resar, The high-mobility group A1 gene up-regulates cyclooxygenase 2 expression in uterine tumorigenesis, Cancer Res. 67 (9) (2007) 3998–4004.

[15] L. Su, Z. Deng, F. Leng, The mammalian high mobility group protein AT-hook 2 (HMGA2): biochemical and biophysical properties, and its association with Adipogenesis, Int. J. Mol. Sci. 21 (10) (2020).

[16] Y.C. Wang, J.S. Liu, H.K. Tang, J. Nie, J.X. Zhu, L.L. Wen, Q.L. Guo, miR-221 targets HMGA2 to inhibit bleomycin-induced pulmonary fibrosis by regulating TGF-beta1/Smad3-induced EMT, Int. J. Mol. Med. 38 (4) (2016) 1208–1216.

[17] P. Savagner, I. Karavanova, A. Perantoni, J.P. Thiery, K.M. Yamada, Slug mRNA is expressed by specific mesodermal derivatives during rodent organogenesis, Dev. Dyn. 213 (2) (1998) 182–187.

[18] Z. Li, X. Wu, J. Li, S. Yu, X. Ke, T. Yan, Y. Zhu, J. Cheng, J. Yang, HMGA2-Snai2 axis regulates tumorigenicity and stemness of head and neck squamous cell carcinoma, Exp. Cell Res. 418 (1) (2022), 113271.

[19] Y. Lin, C. Dong, B.P. Zhou, Epigenetic regulation of EMT: the Snail story, Curr. Pharm. Des. 20 (11) (2014) 1698–1705.

[20] W. Zhou, K.M. Gross, C. Kuperwasser, Molecular regulation of Snai2 in development and disease, J. Cell Sci. 132 (23) (2019).

[21] Y. Liu, H. Lin, L. Jiang, Q. Shang, L. Yin, J.D. Lin, W.S. Wu, L. Rui, Hepatic Slug epigenetically promotes liver lipogenesis, fatty liver disease, and type 2 diabetes, J. Clin. Invest. 130 (6) (2020) 2992–3004.

[22] Y. Li, Z. Zhao, C. Xu, Z. Zhou, Z. Zhu, T. You, HMGA2 induces transcription factor Slug expression to promote epithelial-to-mesenchymal transition and contributes to colon cancer progression, Cancer Lett. 355 (1) (2014) 130–140.

[23] D.E. Kleiner, E.M. Brunt, M. Van Natta, C. Behling, M.J. Contos, O.W. Cummings, L. D. Ferrell, Y.C. Liu, M.S. Torbenson, A. Unalp-Arida, M. Yeh, A.J. McCullough, A. J. Sanyal, N., Nonalcoholic steatohepatitis clinical research, design and validation of a histological scoring system for nonalcoholic fatty liver disease, Hepatology 41 (6) (2005) 1313–1321.

[24] R. Al Zarzour, M. Ahmad, M. Asmawi, G. Kaur, M. Saeed, M. Al-Mansoub, S. Saghir, N. Usman, D. Al-Dulaimi, M. Yam, *Phyllanthus Niruri* Standardized Extract Alleviates the Progression of Non-Alcoholic Fatty Liver Disease and Decreases Atherosclerotic Risk in Sprague–Dawley Rats, Nutrients 9 (7) (2017).

[25] L. Barbier-Torres, K.A. Fortner, P. Iruzubieta, T.C. Delgado, E. Giddings, Y. Chen, D. Champagne, D. Fernandez-Ramos, D. Mestre, B. Gomez-Santos, M. Varela-Rey, V.G. de Juan, P. Fernandez-Tussy, I. Zubiete-Franco, C. Garcia-Monzon, A. Gonzalez-Rodriguez, D. Oza, F. Valenca-Pereira, Q. Fang, J. Crespo, P. Aspichueta, F. Tremblay, B.C. Christensen, J. Anguita, M.L. Martinez-Chantar, M. Rincon, Silencing hepatic MCJ attenuates non-alcoholic fatty liver disease (NAFLD) by increasing mitochondrial fatty acid oxidation, Nat. Commun. 11 (1) (2020) 3360.

[26] M. Dhibi, F. Brahmi, A. Mnari, Z. Houas, I. Chargui, L. Bchir, N. Gazzah, M. A. Alsaif, M. Hammami, The intake of high fat diet with different trans fatty acid levels differentially induces oxidative stress and non alcoholic fatty liver disease (NAFLD) in rats, Nutr. Metab. (Lond.) 8 (1) (2011) 65.

[27] J. Wu, H. Zhang, H. Zheng, Y. Jiang, Hepatic inflammation scores correlate with common carotid intima-media thickness in rats with NAFLD induced by a high-fat diet, BMC Vet. Res. 10 (2014) 162.

[28] R. Reeves, Structure and function of the HMGI(Y) family of architectural transcription factors, Environ. Health Perspect. 108 (Suppl. 5) (2000) 803–809.

[29] G. Musso, M. Cassader, R. Gambino, Non-alcoholic steatohepatitis: emerging molecular targets and therapeutic strategies, Nat. Rev. Drug Discov. 15 (4) (2016) 249–274.

[30] D. Schuppan, J.M. Schattenberg, Non-alcoholic steatohepatitis: pathogenesis and novel therapeutic approaches, J. Gastroenterol. Hepatol. 28 (Suppl. 1) (2013) 68–76.

[31] E. Makri, A. Goulas, S.A. Polyzos, Epidemiology, pathogenesis, diagnosis and emerging treatment of nonalcoholic fatty liver disease, Arch. Med. Res. 52 (1) (2021) 25–37.

[32] V.T. Samuel, G.I. Shulman, The pathogenesis of insulin resistance: integrating signaling pathways and substrate flux, J. Clin. Invest. 126 (1) (2016) 12–22.

[33] D.N. Markowski, H.W. Thies, A. Gottlieb, H. Wenk, M. Wischnewsky, J. Bullerdiek, HMGA2 expression in white adipose tissue linking cellular senescence with diabetes, Genes Nutr. 8 (5) (2013) 449–456.

[34] X. Zhou, K.F. Benson, H.R. Ashar, K. Chada, Mutation responsible for the mouse pygmy phenotype in the developmentally regulated factor HMGI-C, Nature 376 (6543) (1995) 771–774.

[35] A. Anand, K. Chada, In vivo modulation of Hmgic reduces obesity, Nat. Genet. 24 (4) (2000) 377–380.

[36] X. Du, Z. Wu, Y. Xu, Y. Liu, W. Liu, T. Wang, C. Li, C. Zhang, F. Yi, L. Gao, X. Liang, C. Ma, Increased Tim-3 expression alleviates liver injury by regulating macrophage activation in MCD-induced NASH mice, Cell. Mol. Immunol. 16 (11) (2019) 878–886.

[37] J. Guechot, R.C. Boisson, J.P. Zarski, N. Sturm, P. Cales, E. Lasnier, A.H.F. Group, AST/ALT ratio is not an index of liver fibrosis in chronic hepatitis C when aminotransferase activities are determinate according to the international recommendations, Clin. Res. Hepatol. Gastroenterol. 37 (5) (2013) 467–472.

[38] F.A. Livero, A. Acco, Molecular basis of alcoholic fatty liver disease: from incidence to treatment, Hepatol. Res. 46 (1) (2016) 111–123.

[39] E. Cobbina, F. Akhlaghi, Non-alcoholic fatty liver disease (NAFLD) - pathogenesis, classification, and effect on drug metabolizing enzymes and transporters, Drug Metab. Rev. 49 (2) (2017) 197–211.

[40] Y. Sumida, M. Yoneda, Current and future pharmacological therapies for NAFLD/ NASH, J. Gastroenterol. 53 (3) (2018) 362–376.

[41] J.A. Menendez, R. Lupu, Fatty acid synthase and the lipogenic phenotype in cancer pathogenesis, Nat. Rev. Cancer 7 (10) (2007) 763–777.

[42] M. Febbraio, D.P. Hajjar, R.L. Silverstein, CD36: a class B scavenger receptor involved in angiogenesis, atherosclerosis, inflammation, and lipid metabolism, J. Clin. Invest. 108 (6) (2001) 785–791.

[43] J. Wei, H. Li, S. Wang, T. Li, J. Fan, X. Liang, J. Li, Q. Han, L. Zhu, L. Fan, R. C. Zhao, Let-7 enhances osteogenesis and bone formation while repressing adipogenesis of human stromal/mesenchymal stem cells by regulating HMGA2, Stem Cells Dev. 23 (13) (2014) 1452–1463.

[44] D.M. Mokhtar, Cellular and stromal elements organization in the liver of grass carp, Ctenopharyngodon idella (Cypriniformes: Cyprinidae), Micron 112 (2018) 1–14.

[45] K. Jin, T. Li, G. Sanchez-Duffhues, F. Zhou, L. Zhang, Involvement of inflammation and its related microRNAs in hepatocellular carcinoma, Oncotarget 8 (13) (2017) 22145–22165.

[46] G. He, M. Karin, NF-kappaB and STAT3 - key players in liver inflammation and cancer, Cell Res. 21 (1) (2011) 159–168.

[47] M. Noureddin, J.M. Mato, S.C. Lu, Nonalcoholic fatty liver disease: update on pathogenesis, diagnosis, treatment and the role of S-adenosylmethionine, Exp. Biol. Med. (Maywood) 240 (6) (2015) 809–820.

[48] A. Ayala, M.F. Munoz, S. Arguelles, Lipid peroxidation: production, metabolism, and signaling mechanisms of malondialdehyde and 4-hydroxy-2-nonenal, Oxidative Med. Cell. Longev. 2014 (2014), 360438.

[49] D.A. Chistiakov, M.C. Killingsworth, V.A. Myasoedova, A.N. Orekhov, Y. V. Bobryshev, CD68/macrosialin: not just a histochemical marker, Lab. Investig. 97 (1) (2017) 4–13.

[50] R. Reeves, D.D. Edberg, Y. Li, Architectural transcription factor HMGI(Y) promotes tumor progression and mesenchymal transition of human epithelial cells, Mol. Cell. Biol. 21 (2) (2001) 575–594.

[51] N. Takaha, L.M. Resar, D. Vindivich, D.S. Coffey, High mobility group protein HMGI(Y) enhances tumor cell growth, invasion, and matrix metalloproteinase-2 expression in prostate cancer cells, Prostate 60 (2) (2004) 160–167.

[52] S.A. Polyzos, J. Kountouras, C. Zavos, Nonalcoholic fatty liver disease: the pathogenetic roles of insulin resistance and adipocytokines, Curr. Mol. Med. 9 (3) (2009) 299–314.

[53] S. Kumar, Q. Duan, R. Wu, E.N. Harris, Q. Su, Pathophysiological communication between hepatocytes and non-parenchymal cells in liver injury from NAFLD to liver fibrosis, Adv. Drug Deliv. Rev. 176 (2021), 113869.

[54] J. Roche, P. Nasarre, R. Gemmill, A. Baldys, J. Pontis, C. Korch, J. Guilhot, S. Ait-Si- Ali, H. Drabkin, Global decrease of histone H3K27 acetylation in ZEB1-induced epithelial to mesenchymal transition in lung Cancer cells, Cancers (Basel) 5 (2) (2013) 334–356.

[55] K. Yoshida, K. Matsuzaki, Differential regulation of TGF-beta/Smad signaling in hepatic stellate cells between acute and chronic liver injuries, Front. Physiol. 3 (2012) 53.

[56] J.B. Kopp, TGF-beta signaling and the renal tubular epithelial cell: too much, too little, and just right, J. Am. Soc. Nephrol. 21 (8) (2010) 1241–1243.

[57] H. Ahmed, M.I. Umar, S. Imran, F. Javaid, S.K. Syed, R. Riaz, W. Hassan, TGF-beta1 signaling can worsen NAFLD with liver fibrosis backdrop, Exp. Mol. Pathol. 124 (2022), 104733.

[58] J. Liu, S.G. Kang, P. Wang, Y. Wang, X. Lv, Y. Liu, F. Wang, Z. Gu, Z. Yang, J. K. Weber, N. Tao, Z. Qin, Q. Miao, C. Chen, R. Zhou, Y. Zhao, Molecular mechanism of Gd@C(82)(OH)(22) increasing collagen expression: implication for encaging tumor, Biomaterials 152 (2018) 24–36.

[59] V.G. Giby, T.A. Ajith, Role of adipokines and peroxisome proliferator-activated receptors in nonalcoholic fatty liver disease, World J. Hepatol. 6 (8) (2014) 570–579.

[60] F. Liu, Smad3 phosphorylation by cyclin-dependent kinases, Cytokine Growth Factor Rev. 17 (1–2) (2006) 9–17.

[61] S.Y. Kyung, D.Y. Kim, J.Y. Yoon, E.S. Son, Y.J. Kim, J.W. Park, S.H. Jeong, Sulforaphane attenuates pulmonary fibrosis by inhibiting the epithelial-mesenchymal transition, BMC Pharmacol. Toxicol. 19 (1) (2018) 13.

[62] H.X. Wang, W.J. Li, C.L. Hou, S. Lai, Y.L. Zhang, C. Tian, H. Yang, J. Du, H.H. Li, CD1d-dependent natural killer T cells attenuate angiotensin II-induced cardiac remodelling via IL-10 signalling in mice, Cardiovasc. Res. 115 (1) (2019) 83–93.

[63] Y. Wang, Y. Le, J.Y. Xue, Z.J. Zheng, Y.M. Xue, Let-7d miRNA prevents TGF-beta1- induced EMT and renal fibrogenesis through regulation of HMGA2 expression, Biochem. Biophys. Res. Commun. 479 (4) (2016) 676–682.

[64] X. Wang, Y. Liu, J. Rong, K. Wang, LncRNA HCP5 knockdown inhibits high glucose-induced excessive proliferation, fibrosis and inflammation of human glomerular mesangial cells by regulating the miR-93-5p/HMGA2 axis, BMC Endocr. Disord. 21 (1) (2021) 134.

[65] V. Bolos, H. Peinado, M.A. Perez-Moreno, M.F. Fraga, M. Esteller, A. Cano, The transcription factor Slug represses E-cadherin expression and induces epithelial to mesenchymal transitions: a comparison with Snail and E47 repressors, J. Cell Sci. 116 (Pt 3) (2003) 499–511.

[66] E. Slabakova, Z. Pernicova, E. Slavickova, A. Starsichova, A. Kozubik, K. Soucek, TGF-beta1-induced EMT of non-transformed prostate hyperplasia cells is characterized by early induction of SNAI2/Slug, Prostate 71 (12) (2011) 1332–1343.